Operating Modes of Sandwiched Light-Emitting Electrochemical Cells

Martijn Lenes, Germà Garcia-Belmonte, Daniel Tordera, Antonio Pertegás, Juan Bisquert, and Henk J. Bolink**

Light-emitting electrochemical cells (LECs) are promising lighting devices in which the redistribution of ionic charges allows for double electronic carrier injection from air-stable electrodes. Uncertainties about the mode of operation are limiting the progress of these devices. Using fast (with respect to the current growth time) but resolutive electrical measurement techniques, the electronic transport mechanism in state-of-the-art sandwiched devices can be monitored as a function of the operation time. The results indicate the formation of doped transport layers adjacent to the electrodes that reduces the extent of the central neutral light-emitting layer where electronic transport is limited by space-charge. Prolonged growth of the doped regions beyond that required for efficient injection should be prevented, as this decreases the efficiency and leads to low luminance devices.

1. Introduction

Electroluminescent molecular devices are becoming a serious alternative to their inorganic analogues as their efficiencies and stabilities have improved dramatically over the last years.[1] The most efficient and stable organic light-emitting devices (OLEDs) are based on a multistack architecture of low-molecular-weight components. As OLEDs use an air-sensitive electrode for efficient electron injection, they require rigorous encapsulation to prevent degradation. Another type of electroluminescent device, referred to as a light-emitting electrochemical cell (LEC), has a much simpler architecture and operates with air-stable electrodes.[2–5] In its simplest form (**Figure 1**), LECs consist of a single active layer composed of an ionic transition-metal complex (iTMC).[6–8] This allows for their preparation using solution-based techniques, which makes them suitable for low-cost and large-area applications. A wide range of emission colors, including white,[9] and efficiencies as high as 36 lm W^{-1} have been reached with iridium(III) iTMCs.[10,11] Additionally, stabilities in excess of 3000 h at an average luminance of 250 cd m^{-2} have been reported for this type of electroluminescent device.[12,13] However, to further advance the performance of LECs, a more thorough understanding of the operating mechanism is necessary. Under application of a bias, the current and luminance slowly increase in a timescale ranging from minutes to hours (see **Figure 2**). This behavior has been generally described in terms of the essential property governing LEC operation, which is the separation of ionic charges.

Although this general picture is widely accepted, uncertainty exists on the quantitative shape of ionic distribution and, more importantly, about the properties of the electronic current. Two principal models, the electrochemical model,[2,14] and the electrodynamic model,[15,16] propose somewhat different mechanisms. They differ fundamentally in that the electrochemical model assumes that charge injection is promoted by the doping of the material adjacent to the electrodes, whereas the electrodynamic model assumes a strong decrease in the injection barrier by the accumulation of ions at the interface. In the electrochemical model, the p- and n-doped regions increase with time, and the applied potential drops over the remaining intrinsic region between these doped zones. According to this model, light emission occurs at the zone where the p- and n-doped regions coincide. The dynamic model predicts that the entire electric field drops over a thin electrical double layer at the electrode interfaces, and light emission occurs in the bulk of the film. Recently, several works appeared in which evidence for either one or both of these models is presented.[17–20] In these publications, the potential profile was monitored using Kelvin probe techniques. These studies, however, generated further scientific debate.[21,22] Part of the reason for this ambiguity is that the experiments were performed on planar devices using interdigitated electrodes with spacings ranging from several to hundreds of micrometers. This is much larger than the interelectrode distance in sandwiched devices (typically <200 nm), for which the best performances are achieved.[3,12,13,23,24] As Kelvin probe is a surface-contact technique, it cannot be applied to probe the potential profile in sandwiched devices.

Dr. M. Lenes, D. Tordera, A. Pertegás, Dr. H. J. Bolink
Instituto de Ciencia Molecular
Universidad de Valencia
PO Box 22085, ES-46071 Valencia, Spain
E-mail: henk.bolink@uv.es
Dr. H. J. Bolink
Fundación General de la Universidad de Valencia
PO Box 22085, ES-46071 Valencia, Spain
Prof. G. Garcia-Belmonte, Prof. J. Bisquert
Photovoltaic and Optoelectronic Devices Group
Departament de Física
Universitat Jaume I
ES-12071 Castelló, Spain
E-mail: bisquert@fca.uji.es

DOI: 10.1002/adfm.201002587

© 2011 WILEY-VCH Verlag GmbH & Co. KGaA, Weinheim

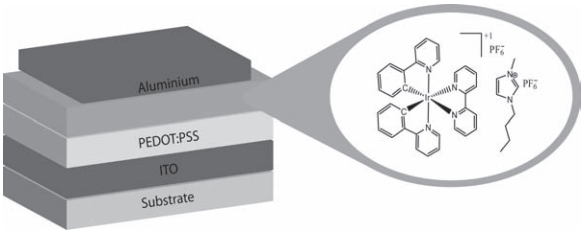

Figure 1. Layout of the LEC and the chemical structures of the iTMC and the ionic liquid used in the active layer.

In this work we study state-of-the-art sandwiched LECs based on an ionic iridium complex using fast current-density and luminance versus voltage scans and impedance spectroscopy, both as a function of operation time. These measurements show that LECs are initially governed by large injection barriers for holes and electrons and, with time, show all the features of bulk limited transport typical for standard OLEDs. It is demonstrated that the charge transport in the undoped (neutral) region is space-charge limited (SCL). From these results, the formation of p- and n-doped regions adjacent to the electrodes is deduced. A new model is proposed that encompasses these findings. This model explains previous observations in LECs, such as the trend of a decreased stability when the turn-on time is reduced by adding extra ions or applying a higher bias.[8]

2. Device Manufacture

All studies presented in this article are performed on sandwiched LECs (Figure 1a), which were prepared by spin coating a thin layer (80 nm) of poly(3,4-ethylenedioxythiophene)–poly(styrenesulfonate) (PEDOT:PSS) on top of a patterned indium tin oxide (ITO) coated glass substrate followed by the active layer (120 nm). This layer consists of bis(2-phenylpyridine-*C,N*)(2,2′-bipyridine-*N,N*′)iridium(III) hexafluorophosphate $[Ir(ppy)_2(bpy)]^+(PF_6^-)$, mixed with the ionic liquid 1-butyl-3-methylimidazolium hexafluorophosphate, $(BMIM^+)(PF_6^-)$ at a molar ratio of 3:1. This ratio was selected to allow for a full analysis within 24 h.[25] Aluminium was used as the top electrode contact.

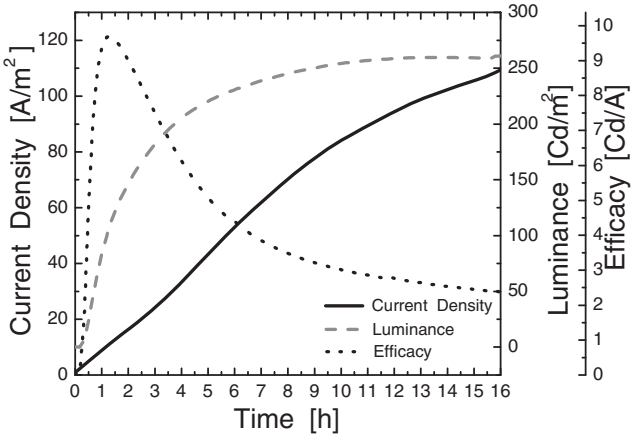

Figure 2. Current density (J, A m^{-2}), luminance (cd m^{-2}) and efficacy (cd A^{-1}) versus time for the sandwiched LEC during fixed voltage operation at 3.5 V.

LECs are generally characterized by applying a fixed voltage and monitoring the current density (J) and luminance (L) over time. Figure 2 shows such a measurement on our iTMC-based LEC, exhibiting the typical features of a LEC: an increase in J over time that saturates, and a luminance which initially increases but after a certain time decreases. The device efficacy, defined as the ratio between luminance and current density, hence shows a maximum at a time in which the luminance is still increasing, a feature which will be discussed in detail later.

As mentioned above, the usual views of LEC operation assume that the slow response observed in Figure 2 is associated with ionic movement towards the metal contacts.[2,14,15] This suggests a very strong separation of the timescales for ionic and electronic phenomena, which constitutes an excellent opportunity for the in situ monitoring of both ionic and electronic properties of the device. In this article, specifically in situ electrical measurement techniques are applied that probe the electronic properties of the device fast enough to not disturb the ionic distribution. In this way, we probe the state of the devices at different times and are able to derive an integral model that explains the experimental results.

3. Measurements

Information on the electronic current, which ultimately governs the luminescence, can be obtained through current-density and luminance versus voltage (JL–V) measurements, the primary analytic technique for conventional light-emitting devices. The very nature of LECs, however, poses difficulties in acquiring these characteristics, since the application of a voltage results in the movement of ionic charges and therefore changes the state of the device. For this reason, JL–V characteristics using slow scan rates as previously reported are unsuitable for our purposes as they resemble characteristics of different ionic distributions for each voltage.[14,26,27] Thus far, only fast (with respect to the ionic movement) JL–V characteristics of LECs with fixed junctions, where the mobile ions are frozen-in or are chemically fixed, have been reported.[24,28–30] These experiments have shown that JL–Vs of fresh LECs are featureless, whereas after poling and fixing they resemble those of standard OLEDs. A thorough investigation of how LECs evolve from the initial state to the highly luminescent state, however, is currently lacking.

To be able to perform JL–V analysis on dynamic LECs, a method was developed that consists of applying a fixed voltage and monitoring the current density and luminescence over time while performing short rapid JL–V scans at set intervals. For the experiment it is crucial that there is no ionic movement during the JL–V scans, as we are interested in the electronic characteristics of the device for a given ionic distribution. Any movement of ions during the JL–V scan will interfere with the fixed-voltage operation. To achieve this, the JL–V scans should fulfil the following conditions: a) they have to be done at a high scan rate (2.5 V s^{-1}), b) they should not significantly go below the iTMC bandgap, and c) they have to be recorded in such a way that the device is never in an off-state between fixed-voltage

© 2011 WILEY-VCH Verlag GmbH & Co. KGaA, Weinheim

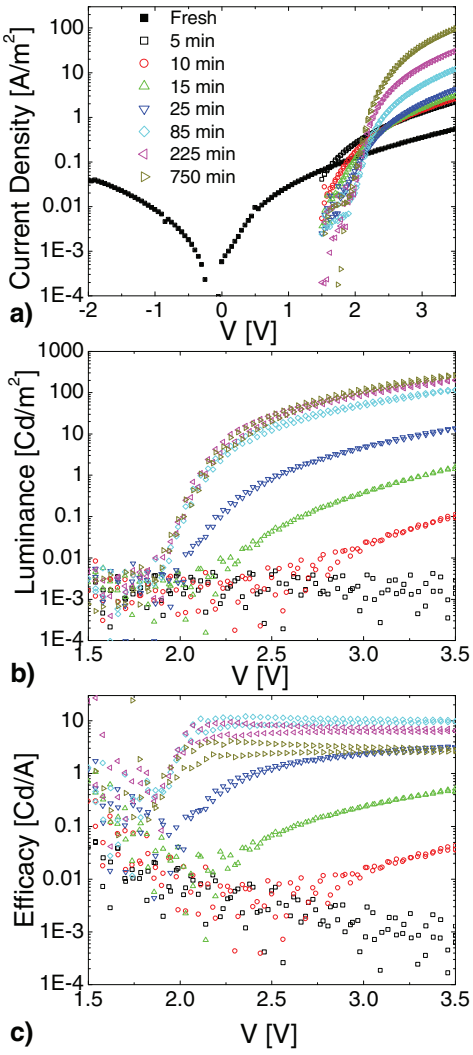

Figure 3. Current density (a), luminance (b), and efficacy (c) versus voltage at different times during fixed-voltage (3.5 V) operation of the sandwiched LEC.

and *JL–V* operations. When these conditions are met, the *JL–V* characteristics show no hysteresis and the current and light output are identical before and after the scan, both indicating that no redistribution of ions has occurred during the *JL–V* sweep. **Figure 3** shows the current-density, luminance, and efficacy versus voltage characteristics acquired at various times during the lifetime measurement depicted in Figure 2. At the beginning of the measurement, the LEC operation is completely dominated by the electron and/or hole injection barrier(s). The *J–V* characteristic is featureless and no light is detected, indicating the measured current is due to local shorts, ionic movement, and/or unipolar injection. Upon the application of a constant voltage of 3.5 V, the device current starts to increase and after 10 min light is detected. At this point, the device shows a high turn-on voltage for light, and the current efficacy is strongly voltage-dependent, both indicating the presence of significant injection barriers. During the next 75 min, the device shows a strong increase in current and light output (Figure 2), and a decrease of the turn-on voltage for light emission (Figure 3). This behavior can be accounted for by both the electrodynamic and the electrochemical models by the accumulation of ions at the interface reducing the injection barriers. After 85 min a key point in the device characteristics is reached. At this point, the turn-on voltage for light emission reaches a minimum and the efficacy has become voltage-independent. Both these features indicate that, at this point, the device is no longer injection-limitied. Yet, without changing the driving voltage, an additional increase in current density of one order of magnitude and an increase in light output by a factor of two is observed at times longer than 85 min.

In bulk-limited OLEDs, the double carrier current density is space-charge limited (partially lifted due to the overlap of holes and electrons, depending on the recombination strength) and can be described by

$$J = \alpha \frac{V^2}{x_n^3} \tag{1}$$

with x_n being the effective layer thickness and α being a coefficient depending on the dielectric constant, electron and hole mobility, and bimolecular recombination rate.[31] In **Figure 4**, the current-density versus the effective applied voltage ($V_{eff} = V - V_{bi}$, where V_{bi} is taken as the point where the current deviates from an exponential dependence) is depicted at different operation times.[32] At driving times of 85 min and beyond, the current undeniably follows the typical quadratic dependence on the voltage, indicating that indeed the current is space-charge limited. The observation of an SCL current at times beyond 85 min is an additional indication that the device is no longer injection-limited, corroborating the conclusion drawn earlier in this article.

According to Equation (1), the one order of magnitude increase of device current after 85 min results from a decrease of the effective layer thickness approximately by a factor of two. To estimate the thickness of this effective layer impedance measurements were performed at a fixed voltage of 3.5 V and

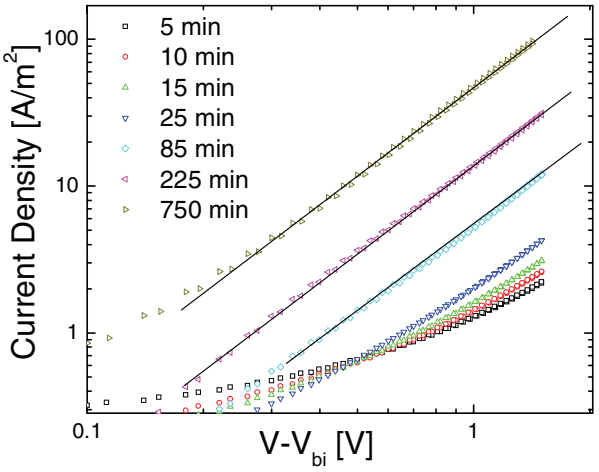

Figure 4. Current density (*J*) versus effective applied voltage ($V - V_{bi}$) at different times during fixed voltage (3.5 V) operation of the sandwiched LEC. The black lines indicate a quadratic dependence.

© 2011 WILEY-VCH Verlag GmbH & Co. KGaA, Weinheim

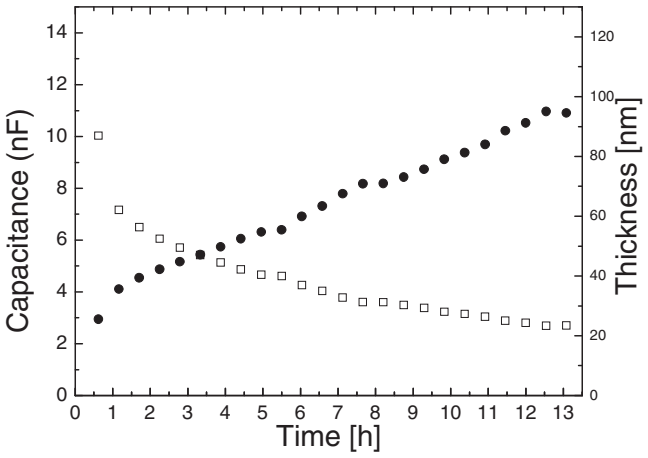

Figure 5. Capacitance (filled circles) and associated thickness of the undoped region (open squares) versus time for the sandwiched LEC during fixed voltage operation at 3.5 V.

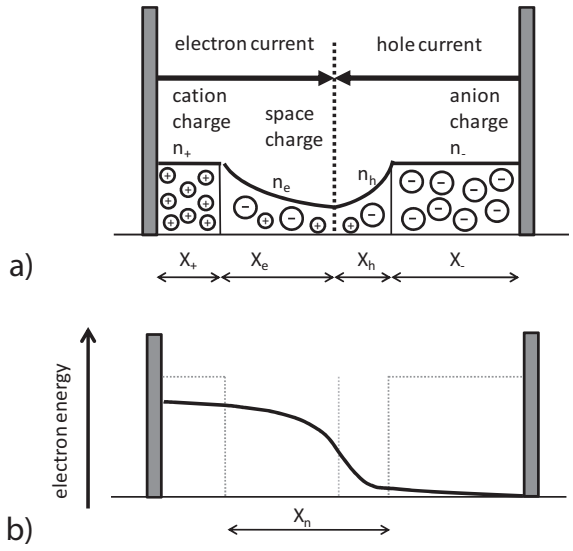

Figure 6. Schematic distribution of a) carrier distribution and b) potential (electron energy) distribution in a model LEC. x^+ and x^- are ohmic regions for electron and hole transport. x_n is a region of ion charge neutrality, where the fields are created by electronic space charge. The recombination zone is the vertical line.

different operation times. **Figure 5** shows the capacitance of the LEC, deduced from the high-frequency part of the spectrum (excluding influences of ionic movements), over time, showing an increase from 2.1 to 11 nF after 12.5 h.

The capacitance directly probes the effective layer as described by the expression

$$C = \varepsilon / x_n \quad (2)$$

where ε is the dielectric constant. The increase in capacitance observed in Figure 5 can therefore be directly related to a decrease in the effective thickness from 67 nm at 85 min to 26 nm at 12.5 h, close to the expected factor of 2 from the increase in device current. Hence, a third-order dependence on thickness is also observed, in line with a space-charge limited current.

4. Discussion

Figure 6 provides a brief description of the model that emerges from these observations. As postulated by the electrochemical model, at driving voltages above the bandgap of the semiconductor, the separation of ionic charges leads to the formation of p- and n-doped regions. It has been suggested that these regions touch at the interface, forming a p–n junction.[18] In contrast to this, we assume that the central region is ionically neutral and electronic carrier transport in this region is limited by space-charges, corroborated by the results mentioned above. These are rather standard features of physical models for OLEDs.[33] Using an analytic formulation of this LEC model, described in the Supporting Information (SI), we derive a potential distribution (Figure 3b) quite similar to that obtained using Kelvin-probe measurements as reported by Matyba et al.[18]

We have thus demonstrated that the LECs described here show a transition from an injection-limited state to a state in which good and balanced injection occurs. After this transition a further increase in current occurs, which implies a reduction in the thickness of the neutral region due to a continuous growth of the doped layers. The current through the neutral region is shown to follow an SCL behavior typical of normal OLEDs, characterized by a quadratic dependence on voltage and a third-order dependence on thickness. The question now remains as to why the efficiency of the device decreases after the p-doped/intrinsic (undoped)/n-doped (p–i–n) geometry is formed (Figure 6). In highly efficient p–i–n OLEDs, in which the doped regions are obtained by reacting the transport molecules with a suitable oxidant or reductant, the emitting layer is separated from the doped layers by additional undoped exciton-blocking layers.[34] In LECs, a similar geometry is formed during operation; however, here the neutral emitting layer is in direct contact to the p- and n-doped regions. In iTMC-based LECs, light emission occurs via phosphorescence originating from long-living triplet excitons. The formation of doped regions adjacent to the neutral emitting layer allows for the quenching of a part of these excitons. The amount of quenched excitons increases as the neutral layer thickness decreases over time, resulting in a significant reduction of the luminance.[35] The fact that the maximum efficacy is reached at the same time as when the device is no longer injection-limited implies that already at this operation time quenching effects start to reduce the device performance. We note that switching the device off for several minutes after reaching the maximum efficiency and re-applying the bias voltage results in the recuperation of the maximum efficacies and luminance levels. This demonstrates that the observed luminance decrease is primarily caused by the quenching of excitons and not due to a permanent degradation reaction of the emitting complexes or breakdown at the contact. The model proposed in this work thus explains previous observed results on the relation between the turn-on time and the stability of LECs when the active layer contains more or smaller ions or when the driving voltage is higher.[8] Both with more or smaller ions or with a higher applied bias, the extension of the doped regions progresses faster, leading to a faster

© 2011 WILEY-VCH Verlag GmbH & Co. KGaA, Weinheim

reduction of the injection barrier and, at the same time, to a faster narrowing of the neutral layer and, hence, to a decrease in luminance. Additionally, as we established that the transport in the neutral layer is space-charge limited, models developed for this type of transport can be used to determine the electron and hole mobilities of the iTMC-based materials in single carrier devices. Such knowledge is essential to further optimize the performances of LECs, for example by employing blends of iTMCs.

The above-described operation mechanism implies that LECs are self-limiting. The prolonged growth of the doped regions beyond that required for efficient injection decreases the efficiency and leads to low-luminance devices. In order to maintain the high efficiency levels achieved after turn-on, the movement of ions and associated doping of the active layer needs to be restricted. It has been demonstrated that it is indeed possible to restrict ion movement by means of changing the ionic conductivity through temperature or chemical reactions, and by applying different driving methods.[24,29,30,36–38]

The observations described in this work hold for LECs that are biased at voltages leading to high luminances; that is, for voltages higher than the bandgap of the electroluminescent material and after approximately 10 min of driving times. At shorter times or lower driving voltages it is possible that the redistribution of ions alone (as assumed by the electrodynamic model) is responsible for an initial decrease in the injection barrier. In fact, using fast *JL–V* measurements versus time on our LECs at biases below the bandgap of the iTMC we observe current transients and a reduction of injection barriers as predicted by the electrodynamic model. This is in agreement with recently published numerical studies on LECs.[20]

5. Conclusions

Using rapid current-density and luminance versus voltage scans and impedance analysis at various points during the operation time of state-of-the-art performing sandwiched LECs we have shown that, once the injection limitation has been overcome, the current density is space-charge limited. The continued increase of the current density at a fixed voltage can only be accounted for by a reduction of the neutral region, which implies the formation of highly conductive doped regions at both interfaces. Furthermore, once the injection barriers are overcome, the device can be described by the well studied space-charge limited current models. Continued doping after the injection barrier has been overcome should be prevented to maintain high-performance devices. Most of the previous reported effects on turn-on time and stability can be rationalized in view of these findings and avenues for more efficient and stable LECs are identified.

6. Experimental Section

Bis(2-phenylpyridine-*C*,*N*)(2,2′-bipyridine-*N*,*N*′)iridium(III) hexafluorophosphate, $[Ir(ppy)_2(bpy)]^+$ (PF_6^-) was synthesized according to methods described previously.[25] The sandwiched LECs were prepared as follows: transparent thin films of $[Ir(ppy)_2(bpy)]^+(PF_6^-)$ containing the ionic liquid 1-butyl-3-methylimidazolium hexafluorophosphate at a molar ratio of 3:1 were obtained by spinning from acetonitrile solutions using concentrations of 30 mg mL^{-1} at 1000 rpm for 40 s, resulting in 120 nm-thick films. Prior to deposition of the emitting layer, an 80 nm layer of PEDOT:PSS was deposited to increase the device preparation yield. The film thickness was determined using an Ambios XP1 profilometer. After spinning the organic layers, the samples were transferred to an inert atmosphere glovebox (<0.1 ppm O_2 and H_2O, MBraun) and dried on a hot plate at 80 °C for 1 h. Aluminium metal electrodes (80 nm) were thermally evaporated using a shadow mask under a vacuum ($<1 \times 10^{-6}$ mbar, 1 bar ≈ 100 000 Pa) using an Edwards Auto500 evaporator integrated into an inert atmosphere glovebox.

Lifetime data were obtained by applying a constant voltage over the device and monitoring the current flow (using a Keithley 2400 source meter) and simultaneously the current generated by a Si-photodiode (Hamamatsu S1336–8BK) using a Keithley 6485 pico-amperometer calibrated using a Minolta LS100 luminance meter. Fast current density and luminance versus voltage sweeps were measured using the same Keithley 2400 source meter and a photodiode coupled to the Keithley 6485 pico-amperometer via a labview controlled custom-made protocol. The custom-designed labview program was used to control the equipment and gather the data on a personal computer. The impedance measurements were performed with an Autolab PGSTAT-30 equipped with a frequency analyzer module in the frequency range of 1 to 10^6 Hz. Each frequency sweep takes less than 1 min. The AC oscillating amplitude was as low as 20 mV (root mean square, rms) to maintain the linearity of the response. The geometrical capacitance of the device was evaluated at zero bias, which allows for the determination of the dielectric constant of the active layer $\varepsilon = 3.7$.

The parameter extraction from the impedance spectra is based on two semicircles. The capacitance data reported corresponds to the larger arc which is related to the reduction of the central layer of the device with time. Additional arcs exist exhibiting minor resistance contributions in comparison to the principal one, which are most likely related to series resistances. The total resistance is in all data dominated by the central layer response.

Supporting Information

Supporting Information is available from the Wiley Online Library or from the author.

Acknowledgements

We are grateful to Jorge Ferrando for his assistance with the *JL–V* experiments and to Edwin Constable and Stefan Graber of the University of Basel for supply of the Iridium complex. This work was supported by the European Union (CELLO, STRP 248043), the Spanish Ministry of Science and Innovation (MICINN) (MAT2007–61584, HOPE CSD2007-00007, CSD2007–00010, CTQ2009–08790) and the Generalitat Valenciana under Project PROMETEO/2009/058.

Received: December 8, 2010
Published online: March 14, 2011

[1] S. Reineke, F. Lindner, G. Schwartz, N. Seidler, K. Walzer, B. Lussem, K. Leo, *Nature* **2009**, *459*, 234.
[2] Q. Pei, G. Yu, C. Zhang, Y. Yang, A. J. Heeger, *Science* **1995**, *269*, 1086.
[3] J. Fang, P. Matyba, L. Edman, *Adv. Funct. Mater.* **2009**, *19*, 2671.
[4] Q. Sun, Y. Li, Q. B. Pei, *J. Display Technol.* **2007**, *3*, 211.
[5] O. Inganas, *Chem. Soc. Rev.* **2010**, *39*, 2633.
[6] E. S. Handy, A. J. Pal, M. F. Rubner, *J. Am. Chem. Soc.* **1999**, *121*, 3525.

© 2011 WILEY-VCH Verlag GmbH & Co. KGaA, Weinheim

[7] F. G. Gao, A. J. Bard, *J. Am. Chem. Soc.* **2000**, *122*, 7426.
[8] J. D. Slinker, J. Rivnay, J. S. Moskowitz, J. B. Parker, S. Bernhard, H. D. Abruña, G. G. Malliaras, *J. Mat. Chem.* **2007**, *17*, 2976.
[9] H. C. Su, H. F. Chen, F. C. Fang, C. C. Liu, C. C. Wu, K. T. Wong, Y. H. Liu, S. M. Peng, *J. Am. Chem. Soc.* **2008**, *130*, 3413.
[10] A. B. Tamayo, S. Garon, T. Sajoto, P. I. Djurovich, I. Tsyba, R. Bau, M. E. Thompson, *Inorg. Chem.* **2005**, *44*, 8723.
[11] H. C. Su, C. C. Wu, F. C. Fang, K. T. Wong, *Appl. Phys. Lett.* **2006**, *89*, 261118.
[12] H. J. Bolink, E. Coronado, R. D. Costa, E. Ortí, M. Sessolo, S. Graber, K. Doyle, M. Neuburger, C. E. Housecroft, E. C. Constable, *Adv. Mater.* **2008**, *20*, 3910.
[13] R. D. Costa, E. Orti, H. J. Bolink, S. Graber, C. E. Housecroft, E. C. Constable, *J. Am. Chem. Soc.* **2010**, *132*, 5978.
[14] Q. B. Pei, Y. Yang, G. Yu, C. Zhang, A. J. Heeger, *J. Am. Chem. Soc.* **1996**, *118*, 3922.
[15] J. C. deMello, N. Tessler, S. C. Graham, R. H. Friend, *Phys. Rev. B.* **1998**, *57*, 12951.
[16] J. C. deMello, *Phys. Rev. B.* **2002**, *66*, 235210.
[17] J. D. Slinker, J. A. DeFranco, M. J. Jaquith, W. R. Silveira, Y. Zhong, J. M. Moran-Mirabal, H. G. Graighead, H. D. Abruña, J. A. Marohn, G. G. Malliaras, *Nat. Mater.* **2007**, *6*, 894.
[18] P. Matyba, K. Maturova, M. Kemerink, N. D. Robinson, L. Edman, *Nat. Mater.* **2009**, *8*, 672.
[19] D. B. Rodovsky, O. G. Reid, L. S. C. Pingree, D. S. Ginger, *ACS Nano* **2010**, *4*, 2673.
[20] S. Reenen van, P. Matyba, A. Dzwilewski, R. A. J. Janssen, L. Edman, M. Kemerink, *J. Am. Chem. Soc.* **2010**, *132*, 13776.
[21] G. G. Malliaras, J. D. Slinker, J. A. Defranco, M. J. Jaquith, W. R. Silveira, Y. Zhong, J. M. Moran-Mirabal, H. G. Graighead, H. D. Abruña, J. A. Marohn, *Nat. Mater.* **2008**, *7*, 168.
[22] Q. Pei, A. J. Heeger, *Nat. Mater.* **2008**, *7*, 167.
[23] L. He, J. Qiao, L. Duan, G. Dong, D. Zhang, L. Wang, Y. Qiu, *Adv. Funct. Mater.* **2009**, *19*, 2950.
[24] Y. Shao, X. Gong, A. J. Heeger, M. Liu, A. K. Y. Jen, *Adv. Mater.* **2009**, *21*, 1972.
[25] R. D. Costa, E. Ortí, H. J. Bolink, S. Graber, S. Schaffner, M. Neuburger, C. E. Housecroft, E. C. Constable, *Adv. Funct. Mater.* **2009**, *19*, 3456.
[26] A. Wu, D. Yoo, J. K. Lee, M. F. Rubner, *J. Am. Chem. Soc.* **1999**, *121*, 4883.
[27] H. Rudmann, S. Shimada, M. F. Rubner, *J. Appl. Phys.* **2003**, *94*, 115.
[28] J. Gao, Y. Li, G. Yu, A. J. Heeger, *J. Appl. Phys.* **1999**, *86*, 4594.
[29] J. M. Leger, D. B. Rodovsky, G. P. Bartholomew, *Adv. Mater.* **2006**, *18*, 3130.
[30] C. V. Hoven, H. Wang, M. Elbing, L. Garner, D. Winkelhaus, G. C. Bazan, *Nat. Mater.* **2010**, *9*, 249.
[31] M. A. Lampert, P. Mark, *Current Injection in Solids*, Academic Press, New York **1970**.
[32] V. D. Mihailetchi, P. W. M. Blom, J. C. Hummelen, M. T. Rispens, *J. Appl. Phys.* **2003**, *94*, 6849.
[33] A. Pitarch, G. Garcia-Belmonte, J. Bisquert, H. Bolink, *J. Appl. Phys.* **2006**, *100*, 084502.
[34] K. Walzer, B. Maennig, M. Pfeiffer, K. Leo, *Chem. Rev.* **2007**, *107*, 1233.
[35] P. Pachler, F. P. Wenzl, U. Scherf, G. Leising, *J. Phys. Chem. B* **2005**, *109*, 6020.
[36] H. Rudmann, M. F. Rubner, *J. Appl. Phys.* **2001**, *90*, 4338.
[37] H. Rudmann, S. Shimada, M. F. Rubner, *J. Am. Chem. Soc.* **2002**, *124*, 4918.
[38] Y. Shao, G. C. Bazan, A. J. Heeger, *Adv. Mater.* **2007**, *19*, 365.

© 2011 WILEY-VCH Verlag GmbH & Co. KGaA, Weinheim